Decision making under uncertainty for building thermal energy storage aggregators participating in two-settlement grid markets

Min Gyung Yu[a,1,*], Gregory S. Pavlak[a,1,2]

[a] *The Pennsylvania State University, 104 Engineering Unit A, University Park, PA 16802, USA*

Abstract

Smart cities will need collections of buildings that are responsive to the variation in renewable energy generation. However, an unprecedented level of renewable energy being added to the power grid compounds the level of uncertainties in making decisions for reliable grid operation. Making autonomous decisions regarding demand management requires consideration of uncertainty in the information available for planning and executing operations. Thus, this paper aims to quantitatively analyze the performances of supervisory controllers for multiple grid-integrative buildings with thermal energy storage depending on the quality of information available. Day-ahead planning and real-time model predictive controllers were developed and compared across 50 validation scenarios when given perfect information, deterministic forecasts, and stochastic forecasts. Despite the relatively large uncertainty in the stochastic forecasts, marked improvements were observed when a stochastic optimization was solved for both the day-ahead and real-time problems. This observation underscores the need for continued development in the area of stochastic control and decision-making for future grid-interactive buildings and improved energy management of smart cities.

Keywords: Grid-interactive buildings, Thermal energy storage, Demand side management, Model predictive control, Stochastic optimization

1. Introduction

Promoting sustainable cities is global agenda to preserve our environment and improve our health [1]. Sustainable and smart cities leverage information and communication technology (ICT) for interactive infrastructure and services, which require sophisticated power networks [2]. As smart grids are introduced, the related technologies can help two-way communication in smart cities and encourage a sustainable built environment [3]. Smart cities can achieve sustainability goals with grid integrated technologies such as energy storage, smart buildings, and distributed energy generation [4]. Especially, as buildings consume more than 75% of U.S. electricity and drive up to 80% of the peak demand on the grid [5], the need to address energy use in the buildings sector is paramount to improving energy management of sustainable cities. It is also expected that the energy management and demand response can reduce CO2 emissions by balancing the power and increasing the stability of the power grid [6]

The concept of grid-interactive energy-efficient buildings (GEBs) has been introduced for reducing building energy use and carbon emissions, as well as for promoting reliable grid operations by integrating building efficiency, energy storage, distributed energy generation, and intelligent controls [7]. As an example, grid-interactive buildings can provide load flexibility by shifting energy usage to off-peak times, which can reduce the stress on the electric grid during peak periods and help increase utilization of renewable electricity [8, 9]. To realize such improved operations in practice, intelligent building control systems need access to

*Corresponding author

Email addresses: mzy57@psu.edu (Min Gyung Yu), gxp93@psu.edu (Gregory S. Pavlak)

[1] Department of Architectural Engineering

[2] Penn State Institutes of Energy and the Environment

predictions of uncertain information, such as occupant behaviors, load patterns, weather conditions, and power prices [10]. However, the variations in occupant behavior and weather may cause unexpected building energy demand fluctuation and unreliable energy management [11, 12, 13]. Thus, intelligent supervisory control algorithms must be capable of developing optimal operating strategies, despite this lack of perfect information.

As a partial means of contending with uncertainty, many power system markets have evolved to adopt a two-settlement approach, where the day-ahead market allows for power procurement based on the expected future scenarios before the operating day, and the real-time market allows for balancing the differences between day-ahead decisions and actual conditions.

To help facilitate building aggregator participation in such two-settlement market structures, recent work has proposed an uncertainty-aware transactive control framework for determining optimal energy procurement decisions [14, 15] for a portfolio of buildings with thermal energy storage (TES).Such a supervisory control decision setting has numerous sources of informational uncertainty in both the day-ahead and real-time periods. However neither the energy saving potential nor the economic impact of the supervisory control for the building aggregator depending on the quality of information is known. It is inevitable to leverage qualified information for advanced energy management of smart cities, and there is a need to further evaluate the performance of the decisions based on the quality of the information that is available in each period. Correspondingly, this paper makes the following contributions:

- Develop stochastic day-ahead planning and real-time operation models for an aggregator of commercial building thermal energy storage resources participating in two-settlement grid markets.
- Systematically quantify the value of applying uncertainty-aware methods in each of the market periods.
- Identify that the stochastic controller affords substantial savings over a deterministic approach, but may still make poor decisions under costly low-probability, high-impact scenarios.

This paper is organized as follows: In Section 2, studies on advanced technologies to support grid-interactive buildings are described. In Section 3, the architecture of the supervisory transactive building energy control platform is illustrated. The mathematical formulation for the deterministic optimization, two-stage stochastic optimization problem, and model predictive control problem is presented in Section 4. Case studies and results are highlighted in Section 5 and 6. Finally, the conclusions and discussion are presented in Section 7.

2. Background

One primary requirement for smart cities and grid-integrated predictive building control is the ability to forecast load variation and flexibility to capture stochastic impacts on building-based grid services [16]. Correspondingly, improved forecasting models are one of the most important strategies for advanced energy management to provide better information about building load flexibility in terms of timing, magnitude, and duration. Machine learning algorithms have been widely studied for building load prediction and analysis [17]. Traditional machine learning algorithms, such as artificial neural network (ANN) and support vector machine (SVM), have been extensively studied in short-term building load prediction [18]. The neural networks showed higher forecasting performance [19]. Yang et al. [20] also employed support vector regression and artificial neural networks to provide site-specific weather forecasts. Results showed that the developed machine-learning-driven methods could accurately forecast the temperature at the target building site one hour ahead. Further, recursive least M-estimate (RLM)-based robust projection [21] and auto-regressive moving average with exogenous variables (ARMAX) [22] models have been introduced to predict volatile electricity price and building load with high accuracy and fast computation for real-time operation.

Once forecasts of future information are available, intelligent control algorithms can be designed to produce optimal or near-optimal control decisions despite the uncertainty in the information. For example, taking into account the forecasting scenarios, two-stage stochastic programming has been introduced to

decide day-ahead planning and control decisions for electric grid systems [23]. Two-stage stochastic optimization approach takes the expected operation based on stochastic scenarios into account when making decisions. To fully enable buildings to absorb volatility in the grid, stochastic approaches have been considered in conjunction with transactive controls to allow the intelligent loads and distributed generation to communicate and coordinate [24, 25, 26]. Stochastic transactive control mechanisms have been introduced for optimal charging schemes of electric vehicle (EV) aggregators [24], optimal cooperation of thermal and electrical storage [26], and building demand response programs with distributed energy resources (e.g., on-site photovoltaics generation and EV charging) [25]. Previous researchers have demonstrated that the combination of transactive controls with stochastic programming can successfully achieve energy and cost savings by planning operations in response to information about future conditions. However, there is little research on applying this approach to building portfolios with active thermal energy storage system, and its application to both day-ahead planning and real-time operation is rare.

To respond to uncertainty in real-time operation, model predictive controllers have been integrated with the power grid to allow buildings to better harness available energy flexibility. For example, model predictive control (MPC) was applied to real-time control of building loads and on-site distributed energy resources to provide demand flexibility [10, 27, 28]. The performance of predictive model relies on the quality of the available input information [29]. To further address the real-time fluctuation, stochastic MPC has been proposed for building HVAC systems [30]. Prior studies demonstrated that the stochastic MPC could achieve the lowest operating cost close to the perfect information case by mitigating the uncertainties [31]. Stochastic transactive approaches have also been combined with model predictive controls to counteract the dynamic real-time uncertainties at each time step and improve economic performance [32, 33]. A stochastic MPC for the transactive operation of multiple buildings has been developed and its application demonstrated its effectiveness to respond to the dynamic nature of real-time power prices. The authors demonstrated the effectiveness of the intelligent framework and discussed the application in community-level building clusters [34].

Most of the reviewed works thus far have focused either on analyzing the performance of the controller or evaluating new forecasting models. Several researchers have studied the combined effects of forecasting models and intelligent control models to support grid-interactive buildings. The quality of input data for the control model was investigated in terms of sensor reliability and installed locations, however, there is presently no work that explores the influence of information availability on the performance of supervisory control for multiple buildings with TES participating in two-settlement markets. Exploring the potential of the building portfolio could be a foundation for a new type of markets and services for smart cities. Thus, there is a need to quantify the benefit of the stochastic framework in both day-ahead planning and real-time operation compared to much simpler deterministic models. Here we include a two-stage stochastic formulation for building portfolio participating in two-settlement markets. Then, we systematically compare the impact of utilizing uncertainty-aware controllers versus deterministic controllers in day-ahead planning and real-time operations. Ultimately, this comparison illuminates if/when it is most beneficial to implement uncertainty-aware decision making. In other words, it answers the question of whether or not we need to solve a stochastic DA planning problem, stochastic RT dispatch problem, or both. This work could be inspirational for the scientific community, utility companies and retail business to leverage aggregated control and DR services at community level.

3. Supervisory transactive building energy control framework

In this section, we describe the architecture of the supervisory transactive building energy control (UA-Tx) framework at the aggregator level as shown in Fig. 1. The aggregator consists of multiple buildings with TES as the flexible energy resource. To make planning and control decisions, the aggregator is required to gather information (blue solid line) about building demand, weather conditions, and real-time power prices as illustrated in Fig. 1. The process starts from day-ahead planning to decide on the power that should be procured in the DA market for customers for the following day. Then, during real-time operations, the aggregator utilizes a model predictive controller to modulate the operation of multiple building TES systems to meet the building cooling loads while reducing peak electric demand. In both DA and RT

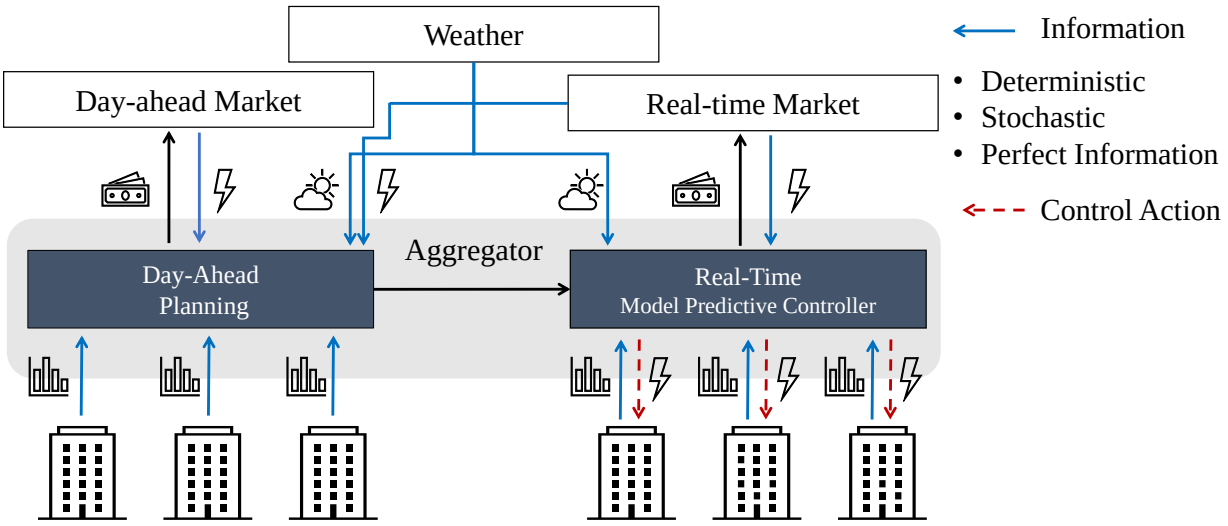

Figure 1: Architecture of the supervisory transactive building energy control platform.

periods, the aggregator makes decisions to reduce operating costs, while adhering to the constraints of the problem. When the building requires more power than what the aggregator expected in the previous day, the aggregator purchases power from the real-time balancing market. When the aggregator has excess power in the real-time market it can also sell back to the market.

The quality of information that is used in both DA and RT decision making can be diverse depending on the forecasting ability, thus, we consider three possible options: "Deterministic", "Stochastic", and "Perfect Information". "Deterministic" denotes using the mean value of a forecasting model, without any information about the potential uncertainty or variation in the forecast. "Stochastic" denotes using the information from many forecasts (i.e., scenarios) generated by sampling a stochastic forecasting model. "Perfect Information" represents having the ability to perfectly forecast the actual condition of the following day.

Fig. 2 illustrates the 9 different combinations of these three options when used in both day-ahead planning and real-time operations. To present a complete analysis, we assume that each of these options could be applied independently in either the day-ahead and real-time periods, or in both periods. For example, we can operate with a perfect forecast in real-time operation even though we had very poor information in day-ahead planning. Likewise, even though we could perfectly decide the day-ahead procurement decision with a high-quality forecast, we might have a very low quality information for real-time operations.

In the "Deterministic" and "Perfect Information" cases, the aggregator makes the power procurement and/or operating decisions by solving a deterministic optimization problem with a single forecast. In the "Stochastic" case, a two-stage stochastic optimization is formulated to solve the day-ahead procurement problem and real-time model predictive controller.

The stochastic MPC problem is approximated by a two-stage stochastic program with the objective of minimizing the sum of operating costs at the current time interval and expected costs for the predicted horizon. Only the first stage decision is implemented, and as the controller steps through time, the building states and forecasting models are updated with the newly observed weather conditions, building patterns, real-time power prices, and new forecasts to solve the next time interval with updated scenarios.

The formulation of the real-time model predictive controller includes a transactive mechanism for the optimal TES operation. Fig. 3 highlights the transactive response established between the aggregator and customers (e.g., Building A, Building B). In this model, the customers submit their current building states, control preferences, and control constraints. The controllable demand range can be defined by the building states and control constraints. Then, the response curve can be drawn connecting the range with the inverse of customers' control preferences as its slope. Therefore, each customer can have its own transactive response curve to communicate their preferences. The aggregator decides the optimal clearing price for each customer

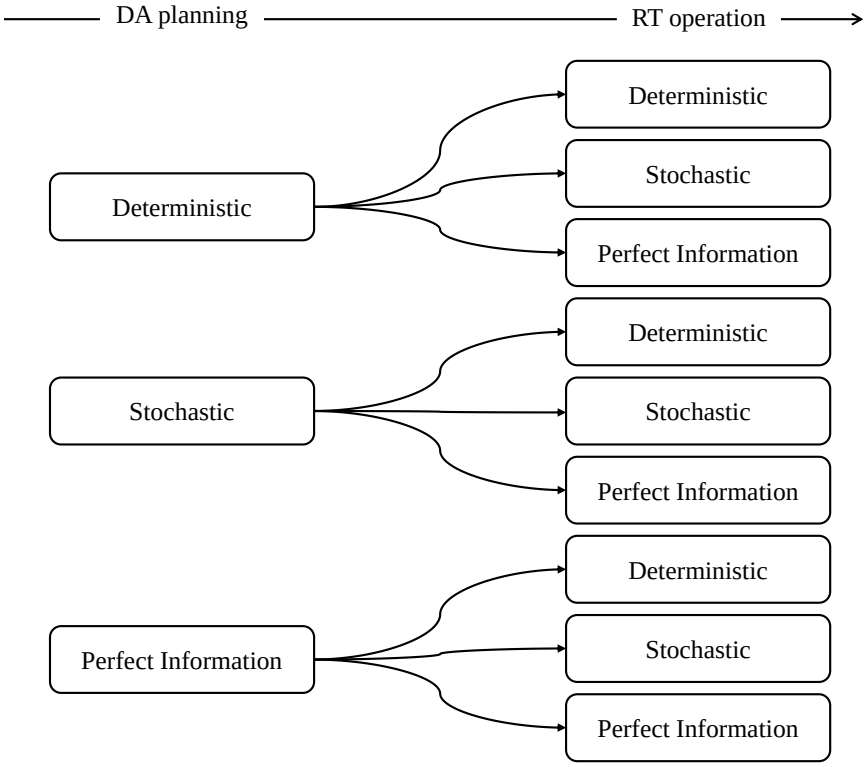

Figure 2: 9 different combinations depending on the quality of information in day-ahead planning and real-time operation.

to provide incentives according to its demand flexibility. Based on the price, the customers implement the corresponding control strategy (i.e, the rate of TES charging or discharging). The process of control actions is described with a red dashed line in Fig. 3.

In Fig. 3, we illustrate two possibilities for control actions depending on the transactive (Tx) clearing prices (λ_{cl}). Building A received a positive value for the clearing price, which drives the control signal to charge TES by operating the dedicated chiller. Building B received a negative value for the clearing price, and the control signal by the response curve operated TES to discharge its thermal energy to meet the building demand in combination with the base chiller. The mathematical formulation is shown in Equations (1) - (3) below,

$$\delta_{b,t} = \theta_b \lambda^{cl}_{b,t} \tag{1}$$

$$q^k_{b,t} = \delta_{b,t} COP_b + q_{b,t} \tag{2}$$

$$p^k_{b,t} = q^k_{b,t}/COP_b + p^{oth}_{b,t} = q_{b,t}/COP_b + \delta_{b,t} + p^{oth}_{b,t} \tag{3}$$

where $\delta_{b,t}$ denotes the control signal for each building; θ_b denotes the customer preference, representing the inverse of the transactive response curve slope; $\lambda^{cl}_{b,t}$ denotes the cleared price determined by the aggregator; $q_{b,t}$ denotes the original heat transfer rate from the base chiller to building demand without the TES operation; $q^k_{b,t}$ denotes the modified heat transfer rate with the TES operation; $p^k_{b,t}$ denotes the actual building electric demand with TES operation; $p^{oth}_{b,t}$ denotes other electric demand by lighting and equipment.

Eq. (1) represents the control signal $\delta_{b,t}$ calculated by the customer preference θ_b and the Tx clearing price $\lambda^{cl}_{b,t}$. The heat transfer rate of the plant system is modified from the original heat transfer rate $q_{b,t}$ with the control variables multiplied by the coefficient of the system (COP) as in Eq. (2). As described earlier, when the building receives a positive value for the control variable $\delta_{b,t}$, the total heat transfer rate of the plant system is increased and charging is implemented by running the dedicated TES chiller to cool

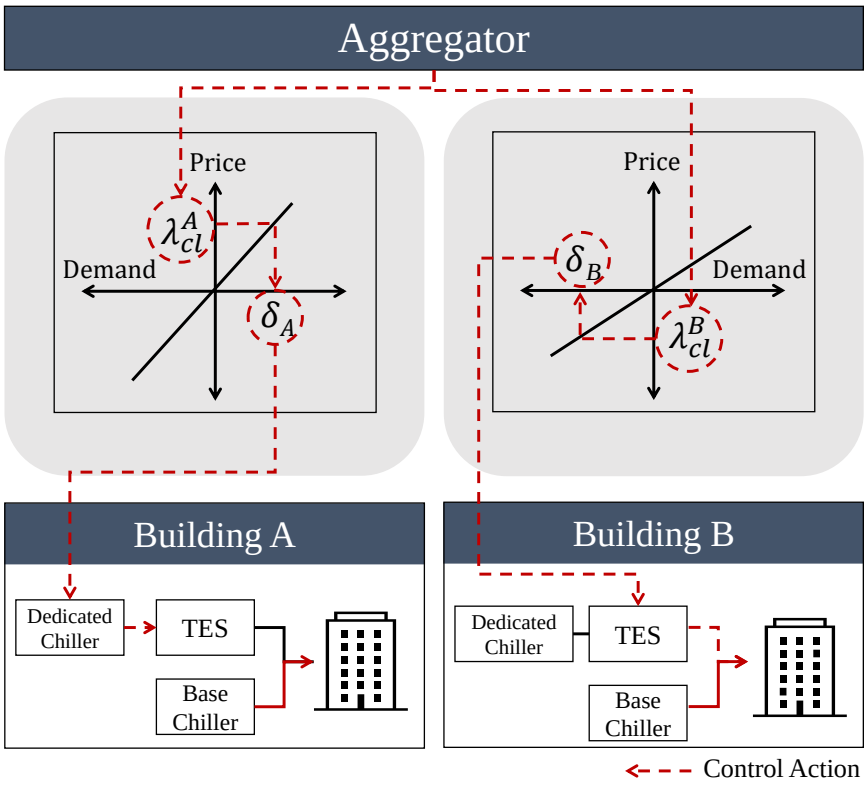

Figure 3: Transactive market model of this work.

the water in the TES tank. When the building receives a negative value for the control variable $\delta_{b,t}$, the total heat transfer rate of the plant system is decreased. In this case, TES is discharging and the base chiller is running lower (or is turned off) to meet the building demand with chilled water flow out of the tank. Finally, Eq. (3) defines the actual power as the sum of the modified heat transfer rate divided by the plant COP plus other electrical loads $p_{b,t}^{oth}$. For computational efficiency, we utilized constant COP for the control-oriented model to represent the COP of the plant [35]. After determining the optimal control decisions using the simplified models, control decisions are implemented in a detailed EnergyPlus model, which captures the effects of part load performance and variable equipment efficiencies.

4. Computational framework

In this section, we begin by presenting the forecasting model and then formally describe the two-stage stochastic programming models used for for day-ahead planning and real-time operation.

4.1. Forecasting model and scenario generation

In this work, we assumed that the forecasting ability of the aggregator can be diverse and we expect that it could influence the overall performance of the control framework. As described in Section 3, three forecasting models were utilized in this study; "Deterministic", "Stochastic", and "Perfect Information". The uncertainties that we consider in the control framework are electric and thermal building demands, weather conditions (outdoor air temperature), and real-time power prices for the following day. To forecast uncertain future conditions, a time series vector auto-regression (VAR) model was developed. Considering co-relations among the building demands, weather conditions, and real-time power price, the regression model was generated by assuming that the forecast of the next time period depends on the patterns from

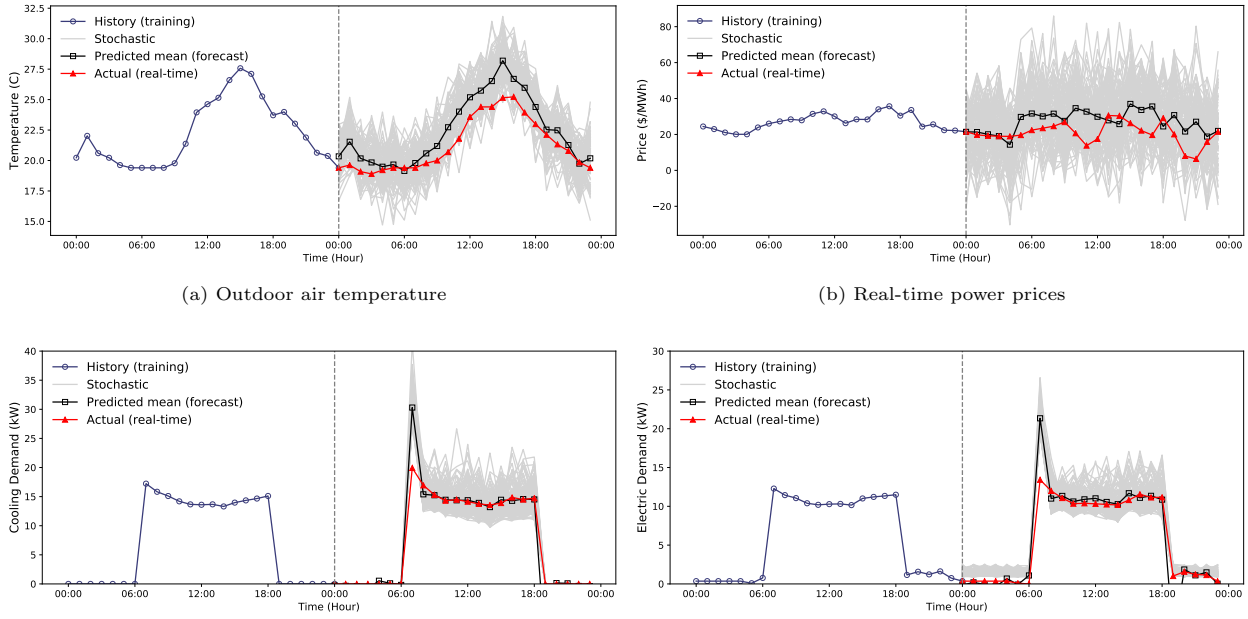

(a) Outdoor air temperature

(b) Real-time power prices

(c) Cooling demand

(d) Electric demand

Figure 4: Comparison between actual and predicted weather, real-time power prices, and cooling demand (6/15).

the lagged time series [36]. In the day-ahead planning, the forecast horizon of the problem was a 24-hour period, and the historical data of 2 weeks was used to generate the VAR model. To remove any seasonal effect and trends from the original historical data, we used the differencing method and removed trends to make stationary time series data. The VAR model was developed using the `statsmodel` package in Python [37], and it produces the minimum mean squared error (MSE) forecasts and forecast interval estimates based on Gaussian variables. The "Deterministic" model uses the mean value of the forecasting model. For the "Stochastic" model, uncertain scenarios are generated using a Monte-Carlo method. "Perfect Information" is having the ability to perfectly forecast the actual condition in the following day. The real-time model predictive controller re-fits the VAR model at every time interval after gathering newly observed data, and the mean forecast values and stochastic scenarios are regenerated to solve for the next time interval. In this work, the historical data of the electricity prices were based on day-ahead and real-time locational marginal prices (LMPs) in the PJM market ComEd zone in 2018 [38], and the historical data of the weather conditions was obtained from the actual weather data from 2018 in Chicago, IL. The historical data of the building demands were generated using the detailed building simulation (EnergyPlus) by differentiating the occupancy schedules and applying actual weather data. Fig. 4 illustrates the comparison between actual and predicted weather, real-time power prices, and cooling demand (June 15th) to visually inspect the model. The predicted forecast models (black solid line with squares) showed a similar pattern to the historical data (blue solid line with circles). The stochastic scenarios (grey solid line) were generated with some variances based on the forecast models as mean values. The stochastic real-time power prices had a wide range of variances. Stochastic building demands tend to have larger values than forecast models. Actual data sets are located in stochastic scenarios.

4.2. Deterministic optimization for day-ahead planning

When "Deterministic" or "Perfect Information" is available, the aggregator can apply deterministic optimization to solve the day-ahead planning problem. The aim of objective function is minimizing electricity procurement cost and expected real-time operating cost, as formulated in Eq. (4).

$$\min \quad (\lambda^{\mathrm{da}})^T\mathbf{x} + \sum_{b\in B}\left((\lambda_b^{cl})^T\delta_b\right) + \lambda^{dr}\sum_{b\in B} z_b - \lambda^{ba}\mathbf{1}^T\sum_{b\in B} p_b^k + (\lambda^{rt})^T(u^+ - u^-)$$
$$+ \eta_1\|u^+\|^2 + \eta_1\|u^-\|^2 + \eta_2\sum_{b\in B} q_b^{ne} + \eta_3\sum_{b\in B} q_b^{ov} + \eta_4 p^{ex} + \eta_5(y_1^2 + y_2^2) \tag{4}$$

$$\text{subject to} \quad 0 \le \mathbf{x} \le \sum_{b\in B} p_b^h, \tag{5}$$

$$p_{b,t}^k = q_{b,t}/COP + \delta_{b,t} + p_{b,t}^{oth} \quad \forall b,t \tag{6}$$

$$0, \pm\lambda_{b,t}^{cl} \le z_{b,t}, \quad \forall b,t \tag{7}$$

$$0 \le u_t^-, u_t^+, y_1, y_2 \quad \forall t \tag{8}$$

$$(u_t^+ - u_t^-) = \sum_{b\in B} p_{b,t}^k - x_t, \quad \forall t \tag{9}$$

$$y_1 - a_1\sum_{b\in B}\sum_{t\in T} p_{b,t}^k \le \mathbf{1}^T\mathbf{x} \le y_2 + a_2\sum_{b\in B}\sum_{t\in T} p_{b,t}^k \tag{10}$$

$$SOC_b^{\min} \le SOC_{b,t} \le SOC_b^{\max} \quad \forall b,t \tag{11}$$

$$\delta_{b,t}COP_b = (SOC_{b,t} - SOC_{b,t-1})CAP_b^{\mathrm{tes}}, \forall b,t \tag{12}$$

$$\delta_{b,t}COP_b \le CAP_b^{ch}, \quad \forall b,t \tag{13}$$

$$\delta_{b,t}COP_b \le (SOC_b^{\max} - SOC_{b,t})CAP_b^{tes}, \quad \forall b,t \tag{14}$$

$$(SOC_b^{min} - SOC_{b,t})CAP_b^{\mathrm{tes}} \le \delta_{b,t}COP_b, \quad \forall b,t \tag{15}$$

$$0 \le q_{b,t}^k, p_{b,t}^k, \quad \forall b,t \tag{16}$$

$$q_{b,t}^{dis} \le 0, \delta_{b,t}COP_b \quad \forall b,t \tag{17}$$

$$0 \le q_{b,t}^{ne}, q_{b,t}^{ov}, p_t^{ex}, \quad \forall b,t \tag{18}$$

$$q_{b,t}^{dis} - CAP_b^{ch2} + q_{b,t} \le q_{b,t}^{ne} \quad \forall b,t \tag{19}$$

$$0 \le \delta_{b,t}COP_b + q_{b,t} + q_{b,t}^{ov}, \quad \forall b,t \tag{20}$$

$$\sum_{b\in B} p_b^k - p_t^{ex} \le p^{peak} \tag{21}$$

where $\mathbf{x} = \left\{\mathbf{x}_t : \forall t\in T\right\}$ represents the power procurement decisions in the day-ahead planning; $\lambda^{\mathrm{da}} = \left\{\lambda_t^{\mathrm{da}} : \forall t\in T\right\}$ denotes day-ahead power price; $\lambda^{\mathrm{rt}} = \left\{\lambda_t^{\mathrm{rt}} : \forall t\in T\right\}$ denotes the power prices in real-time balancing market, λ^{dr} represents the fixed demand response price in transactive market, λ^{ba} is the base electricity price that the customers pay for the power usages to the aggregator; $z_b = \left\{z_{b,t} : \forall t\in T\right\}$ allows for capturing the absolute value of clearing price λ_b^{cl}; $u^+ = \left\{u_t^+ : \forall t\in T\right\}$ and $u^- = \left\{u_t^- : \forall t\in T\right\}$ denote the dummy variables for modeling the deviation between the actual total building demand with TES operation and the procurement; y_1 and y_2 are the dummy variables for modeling the deviation between the daily sum of procured energy and the total daily actual energy use with TES operation; $SOC_b = \left\{SOC_{b,t} : \forall t\in T\right\}$ denotes the state-of-charge (SOC) of TES; CAP_b^{tes}, CAP_b^{ch}, and CAP_b^{ch2} denote the thermal energy storage capacity, dedicated thermal energy storage chiller capacity, and base chiller capacity of the building b, respectively; p_b^h denotes the peak electrical demand of total buildings in historical data; $q_{b,t}^{dis}$ represents TES discharging rate; $q_b^{ne} = \left\{q_{b,t}^{ne} : \forall t\in T\right\}$ denotes the lack of thermal energy to meet building cooling demand q_b; $q_b^{ov} = \left\{q_{b,t}^{ov} : \forall t\in T\right\}$ represents the excessive discharging energy; $p^{ex} = \left\{p_t^{ex} : \forall t\in T\right\}$ denotes the amount of actual power over the peak demand limit p^{peak}; η_1 - η_5 denote the penalty values.

The first term in Eq. (4) denotes the cost for day-ahead power procurement, while the second and third terms represent the incentives that the customer would get by providing demand flexibility. The forth term is the revenue of the aggregator according to the amount of power that the customer used. The fifth term is

the real-time balancing cost based on the procurement decision and actual operation. Terms six thru eleven are related to penalty charges. The sixth and seventh terms are penalty terms for constraining the hourly deviation between actual building demand with TES operation and procurement decision. The eighth term denotes comfort penalty for providing enough thermal energy to the buildings. The ninth term encourages TES to not discharge beyond the plant load to be met. The tenth term denotes the peak limit penalty for limiting the actual power to be below the desired peak limit. The eleventh term charges penalties on the dummy variables to constrain the deviation between the total daily procurement and the daily sum of actual power to be within the desired range.

This planning problem is solved subject to several constraints as in Eq. (5) - (21). Eq. (5) constrains the procured power in the day-ahead planning to be positive and lower than the aggregated peak demand. Eq. (6) defines the actual power by controlling the TES operation. Eq. (7) allows the dummy variable $z_{b,t}$ for representing the absolute value of clearing price. Eq. (8) represents the dummy variables u_t^+, u_t^-, y_1, y_2 to be non-negative values. Eq. (9) denotes the deviation between u_t^+ and u_t^- to be the deviation between the aggregated actual building demands and the procured electricity. Eq. (10) allows the total daily procurement to be between a_1 and a_2% percent of the daily sum of actual power. a_1 and a_2 were set at 0.75 and 1.25, respectively, for this work to reflect a range of ±25%. Eq. (11) limits the SOC levels to be within the specific lower SOC_b^{min} and upper SOC_b^{max} bounds of each building b. Eq. (12) denotes the modified amount of heat transfer rate by the control variable to be equal to the difference in the SOC levels multiplied by the TES capacity. Eq. (13) constrains the heat transfer rate from TES charging to be lower than the dedicated chiller capacity. Eq. (14) represents that the heat transfer rate from TES charging should be lower than the extra capacity of TES. Eq. (15) allows the TES discharging to be less than or equal to the remaining energy in the TES. Eq. (16) requires that the actual thermal and electrical demands be non-negative. Eq. (17) allows the variable $q_{b,t}^{dis}$ to representing TES discharging rate. Eq. (18) represents the non-negative variables $q_{b,t}^{ne}, q_{b,t}^{ov}, p_t^{ex}$ to be used for penalty charges. Eq. (19) denotes the lack of thermal energy $q_{b,t}^{ne}$ from the sum of TES discharging $q_{b,t}^{dis}$ and base chiller CAP_b^{ch2} to meet building cooling demand $q_{b,t}$. Eq. (20) represents the excess TES discharging energy more than the building demand. Eq. (21) denotes the amount of actual power over the peak demand limit.

In this scheme, the building demand q_b and the real-time power price λ^{rt} are from the forecasting model. The day-ahead power prices λ^{da} are known from the markets. When the aggregator operates with the "Deterministic" source, the mean value of forecasting model is applied in the formulation to solve the problem, while the aggregator solves the problem with the actual information of the following day in the "Perfect Information" case.

4.3. Two-stage stochastic optimization for day-ahead planning

When "Stochastic" forecasts are provided, the aggregator solves the day-ahead procurement decisions using a two-stage stochastic optimization. The objective function is formulated to minimize the total sum of procurement costs and expected real-time operation costs based on the set of forecast scenarios as formulated in Eq. (22).

$$\min_{\mathbf{x}} \quad (\lambda^{\mathrm{da}})^T \mathbf{x} + \mathbb{E}\left[\mathcal{Q}(\mathbf{x}, \omega)\right] \tag{22}$$

$$\text{subject to} \quad 0 \leq \mathbf{x} \leq \sum_{b \in B} p_b^h, \tag{23}$$

Two-stage stochastic formulation is differentiated in that it consists of the first term for the day-ahead procurement costs and the seconds term representing the expected real-time operating costs over the set of stochastic scenarios Ω, unlike the objective function of deterministic formulation in Eq. (4). Thus, the variable related to the first stage (first term) is the procurement decision $\mathbf{x}$ that we want to get from the problem-solving, the variables related to the second stage (second term) are for the following day which can be corrected when the actual realization is observed. Therefore, Eq. (23) constrains the variable for the first stage. $\mathcal{Q}(\mathbf{x}, \omega)$ is the optimal value of second-stage problem and the expected value is defined over the set of

scenarios ($\omega \in \Omega$). The problem is to minimize the real-time operating costs, including the penalty charges. The constraints in the second stage problem are limited by first-stage decisions $\mathbf{x}$ as in (24) - (41).

$$\mathcal{Q}(\mathbf{x},\omega) = \min \sum_{b\in B} \left((\lambda^{cl}_{b,\omega})^T \delta_{b,\omega}\right) + \lambda^{dr} \sum_{b\in B} z_{b,\omega} - \lambda^{ba} \mathbf{1}^T \sum_{b\in B} p^k_{b,\omega} + (\lambda^{rt}_{\omega})^T (u^+_{\omega} - u^-_{\omega}) + \eta_1 \|u^+_{\omega}\|^2 + \eta_1 \|u^-_{\omega}\|^2 + \eta_2 \sum_{b\in B} q^{ne}_{b,\omega} + \eta_3 \sum_{b\in B} q^{ov}_{b,\omega} + \eta_4 p^{ex}_{\omega} + \eta_5 (y^2_{1,\omega} + y^2_{2,\omega}) \tag{24}$$

$$\begin{aligned}
\text{subject to} \quad & p^k_{b,t,\omega} = q_{b,t,\omega}/COP + \delta_{b,t,\omega} + p^{oth}_{b,t,\omega} \quad \forall b,t && (25)\\
& 0, \pm\lambda^{cl}_{b,t,\omega} \le z_{b,t,\omega}, \quad \forall b,t && (26)\\
& 0 \le u^-_{t,\omega}, u^+_{t,\omega}, y_{1,\omega}, y_{2,\omega}, \quad \forall t && (27)\\
& (u^+_{t,\omega} - u^-_{t,\omega}) = \sum_{b\in B} p^k_{b,t,\omega} - x_t, \quad \forall t && (28)\\
& y_{1,\omega} - a_1 \sum_{b\in B}\sum_{t\in T} p^k_{b,t,\omega} \le \mathbf{1}^T \mathbf{x} \le y_{2,\omega} + a_2 \sum_{b\in B}\sum_{t\in T} p^k_{b,t,\omega} && (29)\\
& SOC^{\min}_b \le SOC_{b,t,\omega} \le SOC^{\max}_b \quad \forall b,t && (30)\\
& \delta_{b,t,\omega} COP_b = (SOC_{b,t,\omega} - SOC_{b,t-1,\omega}) CAP^{\text{tes}}_b, \forall b,t && (31)\\
& \delta_{b,t,\omega} COP_b \le CAP^{ch}_b, \quad \forall b,t && (32)\\
& \delta_{b,t,\omega} COP_b \le (SOC^{\max}_b - SOC_{b,t,\omega}) CAP^{tes}_b, \quad \forall b,t && (33)\\
& (SOC^{min}_b - SOC_{b,t,\omega}) CAP^{\text{tes}}_b \le \delta_{b,t,\omega} COP_b, \quad \forall b,t && (34)\\
& 0 \le p^k_{b,t,\omega}, \quad \forall b,t && (35)\\
& q^{dis}_{b,t} \le 0 \quad \forall b,t && (36)\\
& 0 \le q^{ne}_{b,t,\omega}, q^{ov}_{b,t,\omega}, p^{ex}_{t,\omega}, \quad \forall b,t && (37)\\
& q^{dis}_{b,t,\omega} \le \delta_{b,t,\omega} COP_b, \quad \forall b,t && (38)\\
& q^{dis}_{b,t,\omega} - CAP^{ch2}_b + q_{b,t} \le q^{ne}_{b,t,\omega}, \quad \forall b,t && (39)\\
& 0 \le \delta_{b,t,\omega} COP_b + q_{b,t,\omega} + q^{ov}_{b,t,\omega}, \quad \forall b,t && (40)\\
& \sum_{b\in B} p^k_b - p^{ex}_{t,\omega} \le p^{peak} && (41)
\end{aligned}$$

In this scheme, the building demand $q_{b,\omega}$ and the real-time power price λ^{rt}_{ω} are from the forecasting models, which are different from the actual realizations in the real-time operation. We assumed that all the expected values $\mathcal{Q}(\mathbf{x},\omega)$ have the same probability in this problem.

4.4. Deterministic model predictive controller for real-time operation

The procurement decision $\mathbf{x}$ in the day-ahead planning is loaded in the model-predictive controller to dispatch the power to the customers as well as to provide demand flexibility by controlling the operation of multiple building TES in real-time operation. When "Deterministic" or "Perfect" information is provided to the aggregator, a deterministic model-predictive controller is used to minimize the real-time operation cost based on the day-ahead procurement decision $\mathbf{x}$ and the actual realization. The formulation is referred the deterministic optimization for day-ahead planning problem as Eq. (42).

$$\min \sum_{b\in B} \left((\lambda^{cl}_b)^T \delta_b\right) + \lambda^{dr} \sum_{b\in B} z_b - \lambda^{ba} \mathbf{1}^T \sum_{b\in B} p^k_b + (\lambda^{rt})^T (u^+ - u^-) + \eta_2 \sum_{b\in B} q^{ne}_b + \eta_3 \sum_{b\in B} q^{ov}_b + \eta_4 p^{ex} \tag{42}$$

In Eq. (42), the control variables are decided at every time interval and last until the next time interval. In this work, we used perfect information to determine the optimal control variable at the current time interval since the time interval of this work is one hour and local loop controllers would modulate within the hour to maintain system performance under the actual realizations. The future horizons of the model use the expected building demand, expected weather condition, and expected power prices. For the constraints, this real-time deterministic controller follows (6) – (9), (11) – (21) for the prediction horizon.

We summarize the deterministic MPC scheme as follows. It starts with updating the building model and the observation history from the previous time step. Based on the updated information, the VAR model is developed and the parameters are re-fit every time interval to generate the mean forecast values for weather, demands, and power prices. The optimal TES control strategy from the MPC controller is implemented in the detailed whole-building simulator (EnergyPlus) for the current time interval to simulate the actual realization. The solutions for the following intervals will be kept on hold. EnergyPlus energy management system (EMS) code implements the control strategies in the model. After executing the control strategy, the actual states are updated at the aggregator level to solve the next time interval. The aggregator iterates the process and the customers operate the TES based on the real-time decisions until the final time interval of the day. The control horizon in the MPC shrinks while moving towards the end of a day.

4.5. Stochastic model predictive controller for real-time operation

When a set of uncertain scenarios for the building demand, weather condition, and real-time power prices is provided to the aggregator, a stochastic model-predictive controller is implemented. Stochastic MPC is formulated as a two-stage problem to capture the expected scenarios for future horizons. Fig. 5 highlights the sketch of the two-stage stochastic model-predictive control framework of this work. The procurement decision $\mathbf{x}$ from day-ahead planning is loaded for the real-time modulation at the aggregator level. The control decision variables δ_1 for the time step $t = 1$ are here-and-now (first stage) decisions that will last until the next time interval $t + 1 = 2$. Second stage variables are wait-and-see (recourse) variables for the following time intervals, which can be corrected when the actual realization is observed. The aggregator carries out the problem to minimize the total expected costs over the prediction horizon as formulated in Eq. (43). Since the operator can modulate the HVAC control depending on the actual building condition regardless of the expected optimal control decisions, this work decided to use perfect information for the first stage decisions.

$$\min \quad f(\delta_b) + \mathbb{E}\left[L(\delta_b, \omega)\right] \tag{43}$$

The first stage (term) in Eq. (43) is the cost of the current time interval and the second stage (term) is the expected cost for the following time intervals over all scenarios ($\omega \in \Omega$). The formulation is referred the two-stage stochastic day-ahead planning problem and the first term is formulated as Eq. (44).

$$f(\delta_b) = \sum_{b\in B}\left((\lambda_b^{cl})^T\delta_b\right) + \lambda^{dr}\sum_{b\in B} z_b - \lambda^{ba}\mathbf{1}^T\sum_{b\in B} p_b^k + (\lambda^{rt})^T(u^+ - u^-) + \eta_2\sum_{b\in B} q_b^{ne} + \eta_3\sum_{b\in B} q_b^{ov} + \eta_4 p^{ex} \tag{44}$$

Here, the actual building demand q_b and the actual real-time power prices λ^{rt} for the current time interval are applied to solve the problem. The constraints are limited as in Eq. (25) – (28) and (30) – (41).

$L(\delta_b, \omega)$ is the optimal value of second-stage problem and the expected operating cost in scenario ω can be formulated for the prediction horizon $t' = \{t + 1, \dots T\}$ as Eq. (45). The problem is to minimize the real-time operation costs including the penalty charges according to the decisions, and the constraints are limited as in Eq. (25) – (28) and (30) – (41).

$$\begin{aligned} L(\delta_b, \omega) = \min \sum_{b\in B}\left((\lambda_{b,\omega}^{cl})^T\delta_{b,\omega}\right) + \lambda^{dr}\sum_{b\in B} z_{b,\omega} - \lambda^{ba}\mathbf{1}^T\sum_{b\in B} p_{b,\omega}^k + (\lambda_\omega^{rt})^T(u_\omega^+ - u_\omega^-) + \eta_2\sum_{b\in B} q_{b,\omega}^{ne} \\ + \eta_3\sum_{b\in B} q_{b,\omega}^{ov} + \eta_4 p_\omega^{ex} \end{aligned} \tag{45}$$

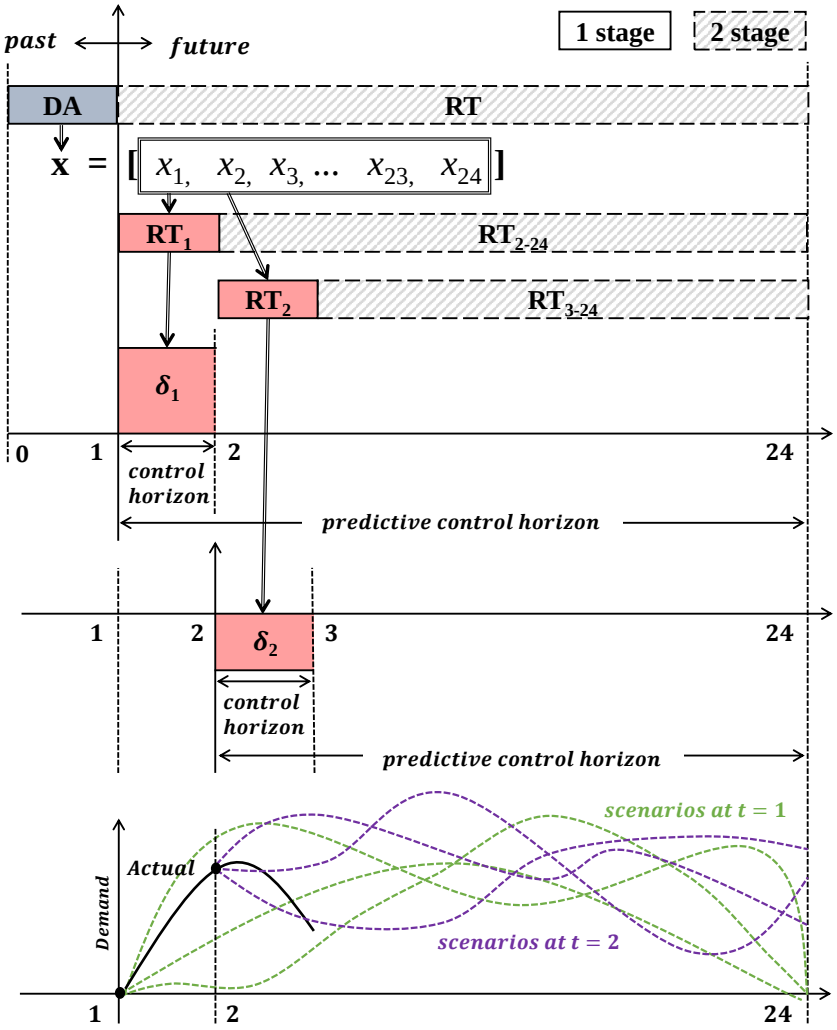

Figure 5: Sketch of two-stage stochastic MPC framework.

As a recourse problem, the variables of Eq. (45) will not be implemented and these can be corrected when the actual disturbance realization is observed.

Unlike the deterministic MPC, the stochastic MPC scheme generates a new set of forecasting scenarios to solve the recourse problem every time interval.

5. Case Studies

This work performed a quantitative analysis for the supervisory controllers for multiple buildings with thermal energy storage to evaluate the influence of the information (mean value of forecasting model, stochastic, perfect information, etc.) on the aggregator level and building level. We will discuss the potential of demand flexibility from the building-based grid services with the proposed control framework. We assumed that there are three levels of information quality in day-ahead planning and real-time operation, respectively. Thus, total of nine cases are considered in this work by differentiating the implementations for the day-ahead planning and real-time operation. In this work, an aggregator's portfolio consisting of 30 office buildings located in Chicago, IL, was utilized and the performance analysis was conducted with a set of 50 validation

scenarios for a week of operation. The building models were developed in our previous research [15] and they were generated by varying the occupancy schedules and parameters of the reference model for dynamic building demands. The performance analysis is focused on evaluating the expected total cost for the aggregator over all the validation scenarios and comparing the decisions among the different implementations. The aggregator procures power in day-ahead market with a prediction horizon of 24 hours (the following day), and it dispatches the power as it modulates the TES control based on the procurement and real-time conditions for every time interval. The time series forecasting model for day-ahead planning is developed once with the prediction horizon (24 hours), and the forecasting model for the real-time model predictive controller is updated at every time interval with the newly observed data. With the forecast model, the mean forecast value is obtained, and the stochastic forecast scenarios are generated using the Monte Carlo sampling based on that. The stochastic problem contains 100 forecast scenarios for each building, thus a total of 511,424 variables and 1,234,000 constraints were considered to solve for 30 buildings. A total of 50 validation scenarios were used to implement this case study. The simulations were run on a server with 2.2 GHz Intel Xeon Processors up to 10 processors and 256 GB RAM. The scripts were developed in Python and the optimization problems were solved using Mosek.

6. Case Study Results

This section is to evaluate the performance of the controller depending on the quality of information with their forecasting model as "Deterministic". "Stochastic", and "Perfect information". Fig. 6 shows the distribution of total aggregator costs for both day-ahead planning and real-time operation including the penalty charges for the set of 50 validation scenarios. Each subfigure of Fig. 6 represents a different combination of the day-ahead (DA) planning and real-time (RT) controller (i.e., green label - deterministic, orange label - stochastic, grey label - perfect information). For example, Fig. 6(b) illustrates the case with "Deterministic" for the day-ahead planning and "Stochastic" for the real-time operation. First, we compared the performances of the cases that used different day-ahead implementations with the same implementation "Perfect Information" for the real-time operation as shown in the box of Fig. 6. Comparing Fig. 6(c), 6(f), and 6(i) shows that stochastic planning is is valuable even if perfect forecasts were available real-time. The deterministic planning had a wider spread of costs among the validation scenarios, and higher average costs. Thus, it was observed that the aggregator may incur large costs from the failure in the day-ahead procurement decision with a lack of information.

Then, we compared the performances of the cases that used the same day-ahead planning but different implementations for the real-time operation to highlight the importance of information in real-time operation. When the day-ahead implementation was the same, the probability distributions for different real-time implementations showed a slightly different pattern. Having the perfect information in the real-time operation showed probabilities at lower costs over the other implementations, while having limited information (deterministic) led to a relatively significant expenditure with the longest tail in real-time operation. Stochastic approach provided expected operation costs close to perfect information, however, its costs were spread wider than in the perfect information case. Especially, the operation based on stochastic programming may result in similar performance as deterministic operation for several scenarios comparing Fig. 6(h) and 6(i)—if perfect information were available DA.

Moreover, among the realistic cases (i.e., excluding perfect information cases), the stochastic approach for both day-ahead planning and real-time operation has the lowest expected costs and less spread in the distribution as observed in Fig. 6(e).

Overall, we observed that the quality of information influences the performances of the aggregator to save operation costs and to avoid penalty charges. It played a much more important role in the real-time operation.

Table 1 summarizes the expected (i.e., average) total costs from the 50 validation scenarios in the case studies. It was observed that the case using the deterministic model for both day-ahead planning and real-time operation showed the largest expected cost, while the case using perfect information for both day-ahead planning and real-time operation showed the lowest expected cost. When keeping the real-time controllers the same, the stochastic model was able to achieve approximately 3.2 - 8.2% operating cost savings over the

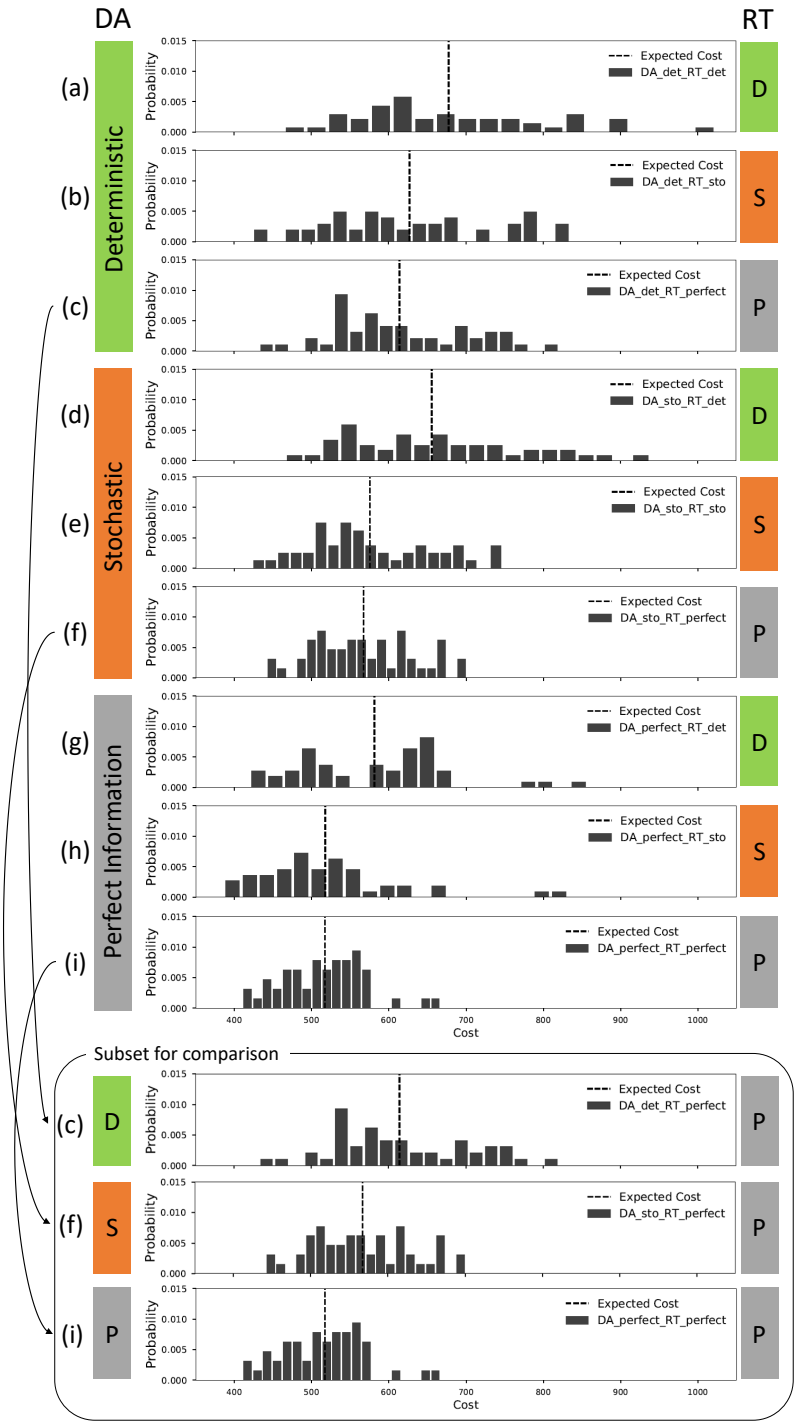

Figure 6: Probability distribution of total cost of the aggregator in case studies (A subset is extracted in the box for comparison).

deterministic case when they were implemented for day-ahead planning (i.e., Det-Det vs Sto-Det, Det-Sto vs Sto-Sto, and Det-Perfect vs Sto-Perfect). For real-time operation, the stochastic model could achieve 7.5 - 12.3 % of cost savings over the deterministic case, when keeping the DA planning method the same (i.e., Det-Det vs Det-Sto, Sto-Det vs Sto-Sto, and Perfect-Det vs Perfect-Sto). The reduction in the costs indicates that considering uncertainties in the planning and operation is quite beneficial for the aggregator profits.

Table 1: Expected total of the aggregator with different combinations of implementations

Day-ahead planning	Real-time operation	Expected cost ($)
Deterministic	Deterministic	677.57
	Stochastic	626.95
	Perfect information	614.13
Stochastic	Deterministic	656.10
	Stochastic	575.56
	Perfect information	567.29
Perfect information	Deterministic	581.38
	Stochastic	517.55
	Perfect information	517.41

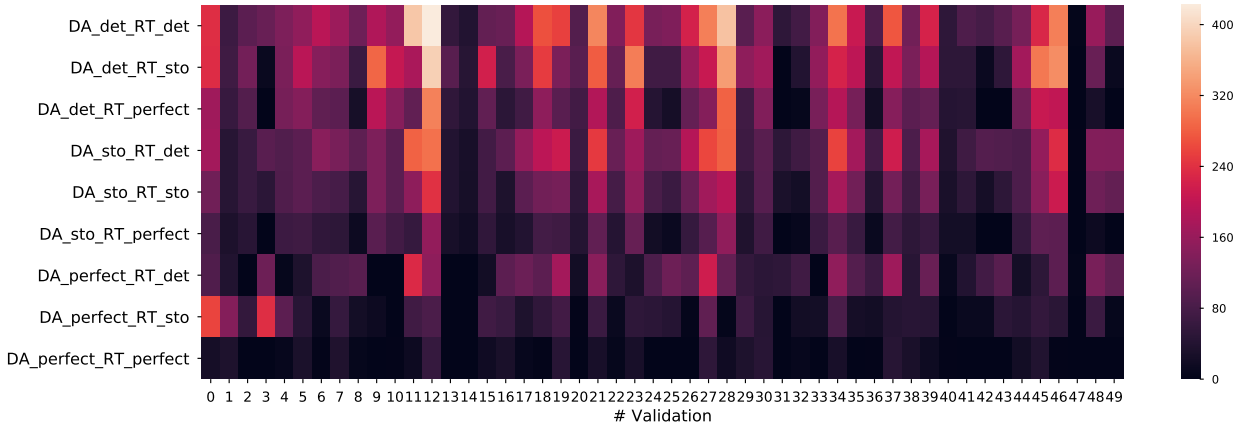

Figure 7: Heatmap showing penalty charges in case studies over the set of validation scenarios.

Fig. 7 provides a heatmap visualizing the penalty charges in the case studies over the set of 50 validation scenarios. In Fig. 7, the variation in color represents the costs from the highest to lowest, thus the darkest color represents the lowest cost and the brightest color illustrates the highest cost. We observed that there is a wide range of color variation for penalty charges when using the "Deterministic" model for day-ahead planning, and it showed the brightest color when it also used "Deterministic" for real-time operation. It supports the observations made from the cost distributions in Fig. 6 that the deterministic case had the longest tail with the highest operating costs. When the stochastic case was used for day-ahead planning, the color variation is relatively darker than the deterministic cases representing fewer penalty charges. When the aggregator utilized the perfect information for day-ahead planning, the penalty charges illustrated the darkest color close to zero except a few scenarios.

Overall, we observed that the penalty charges were decreased as the aggregator changed the model from "Deterministic" to "Stochastic" and "Perfect Information".

In addition to the overall results, one day of one validation scenario is shown in Fig. 8 to highlight the detailed performance comparison when we differentiate the day-ahead plannings while keeping the same real-time implementation (i.e., Perfect information). The representative day is selected based on Fig. 7 having

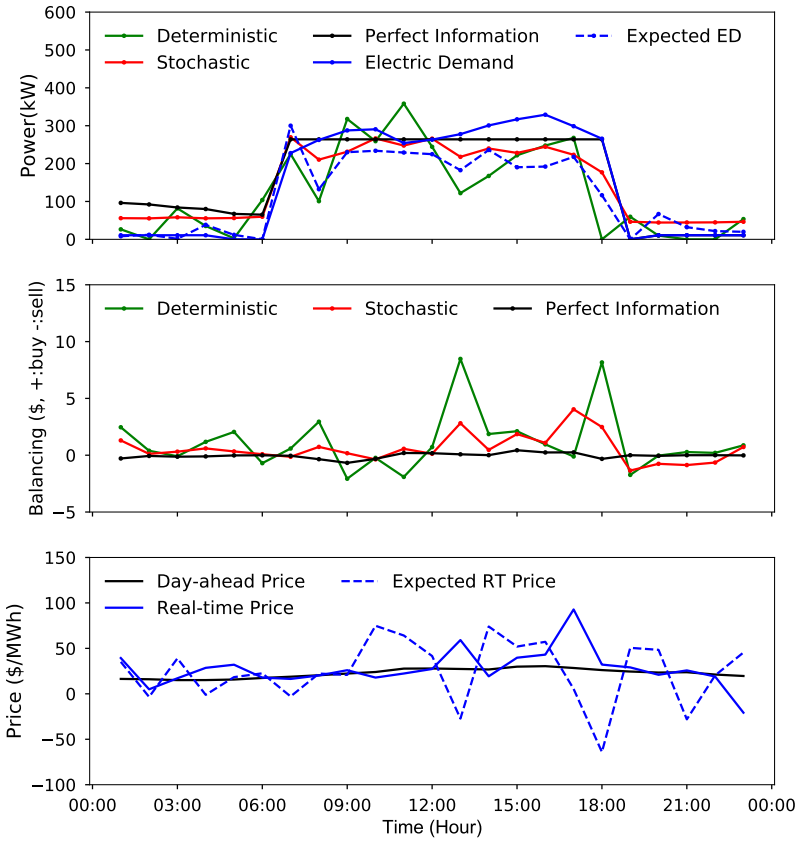

Figure 8: Comparison in day-ahead planning decisions with stochastic, deterministic, and perfect information cases (June 5th Validation No.28).

large differences among the cases. The top subfigure shows the difference in the procurement decisions (Deterministic - green solid line, Stochastic - red solid line, Perfect information - black solid line), original electric demand (blue solid line), and expected electric demand from the deterministic case (blue dashed line). The second subfigure represents the real-time balancing costs based on the day-ahead procurement decisions. Here, the positive balancing cost means that the aggregator purchases the power from the real-time balancing market, while the negative balancing cost represents that the aggregator sells the rest of the power for its profits. The third subfigure illustrates the day-ahead power price (black solid line), expected real-time power price (blue dashed line), and actual real-time power price (blue solid line). Note that the original electric demand in the top subfigure the peaks at 329 kW at 16:00, thus, load shifting or load reduction is needed to meet the peak limit. On the other hand, the expected electric demand that the deterministic case used for decision making was lower than the peak demand limit during operation hours so that the deterministic (green solid line) decided not to purchase enough energy during the early morning hours. On top of that, as shown in the third subfigure, the expected real-time power price for the deterministic model was much more volatile than the actual real-time power price, showing high prices at 9:00-11:00 and the extreme negative price at 18:00. Thus, the deterministic case decided to purchase more than the peak limit at 9:00 and 11:00, but not to purchase any at 18:00 to maximize its profits based on their expected single future scenario. The relatively poor DA decision in the deterministic case resulted in large expenditures at 13:00 and 18:00 and it led to substantial losses on this day. Even though the real-time power price at 18:00 was relatively low, not procuring was financially significant on the total operating costs. For the stochastic case (red solid line), it selected a slightly different procurement strategy as purchasing at 18:00 and it was not a dramatic decision as to the deterministic case. It purchased slightly above the mean of expected electric

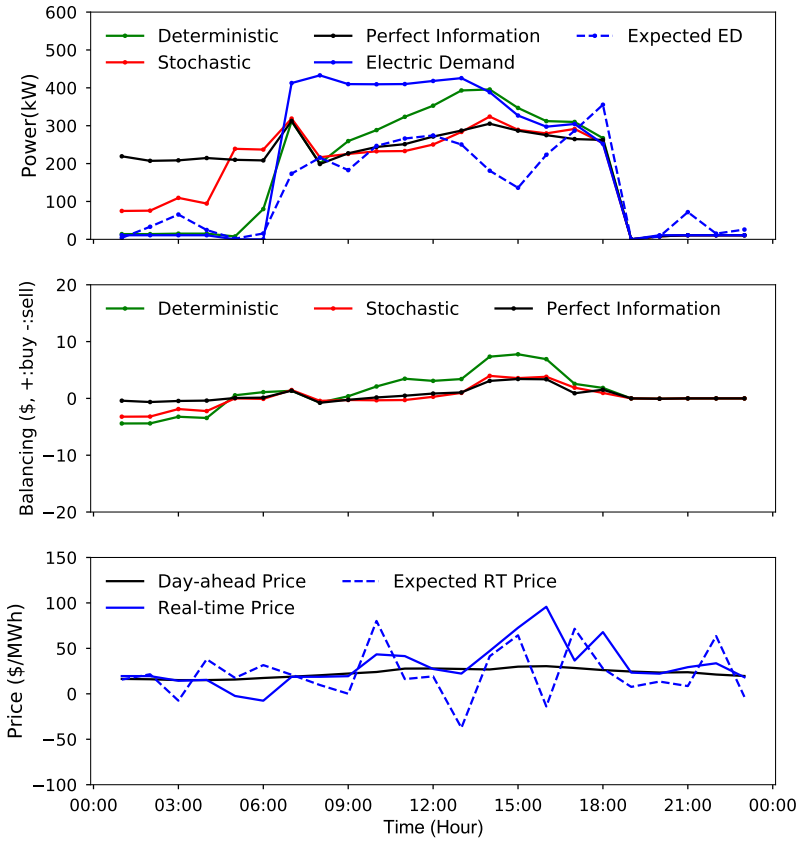

Figure 9: Comparison in real-time operation decisions with stochastic, deterministic, and perfect information (June 5th Validation No. 0).

demand scenarios (blue dashed line) and kept the amount of procurement below the peak limit as shown in the top subfigure. The stochastic case was required to buy power during the real-time operation due to the lack of procurement in the day-ahead market. The second subfigure showed the expenditure at 13:00 and 17:00. Even though the required power at 17:00 was a small amount, the real-time power price by that time was dramatically higher than other times, so that the aggregator ended up paying a high expenditure. When perfect information was available (black solid line), it showed a similar pattern as the stochastic approach and purchased even more at 18:00 as shown in the top subfigure. Since it used perfect information, the second subfigure shows that the aggregator had nearly zero balancing costs. It is expected that the perfect information case made a decision to procure perfectly in the day-ahead market to avoid the influence from much volatile real-time power price. In addition, we observed that about a 17.9% reduction in peak from 329 kW to 270 kW. Overall, the deterministic model utilized only the mean value when decision-making, so that the only expected scenario had a significant influence on the decision, while the stochastic model was able to consider a wide range of variability at each hour to avoid the extreme expenditure.

Fig. 9 highlights the comparison in real-time operation when applied the same perfect information for the day-ahead planning. The top subfigure shows the difference in the real-time operation decisions (Deterministic - green solid line, Stochastic - red solid line, Perfect information - black solid line), original electric demand (blue solid line), and expected electric demand from the deterministic case (blue dashed line). The second subfigure represents the real-time balancing costs based on the day-ahead procurement decisions. The third subfigure illustrates the day-ahead power price (black solid line), expected real-time power price (blue dashed line), and actual real-time power price (blue solid line). On this day, the original building electric demand (before TES operation, blue solid line) was above the peak limit (270 kW), thus,

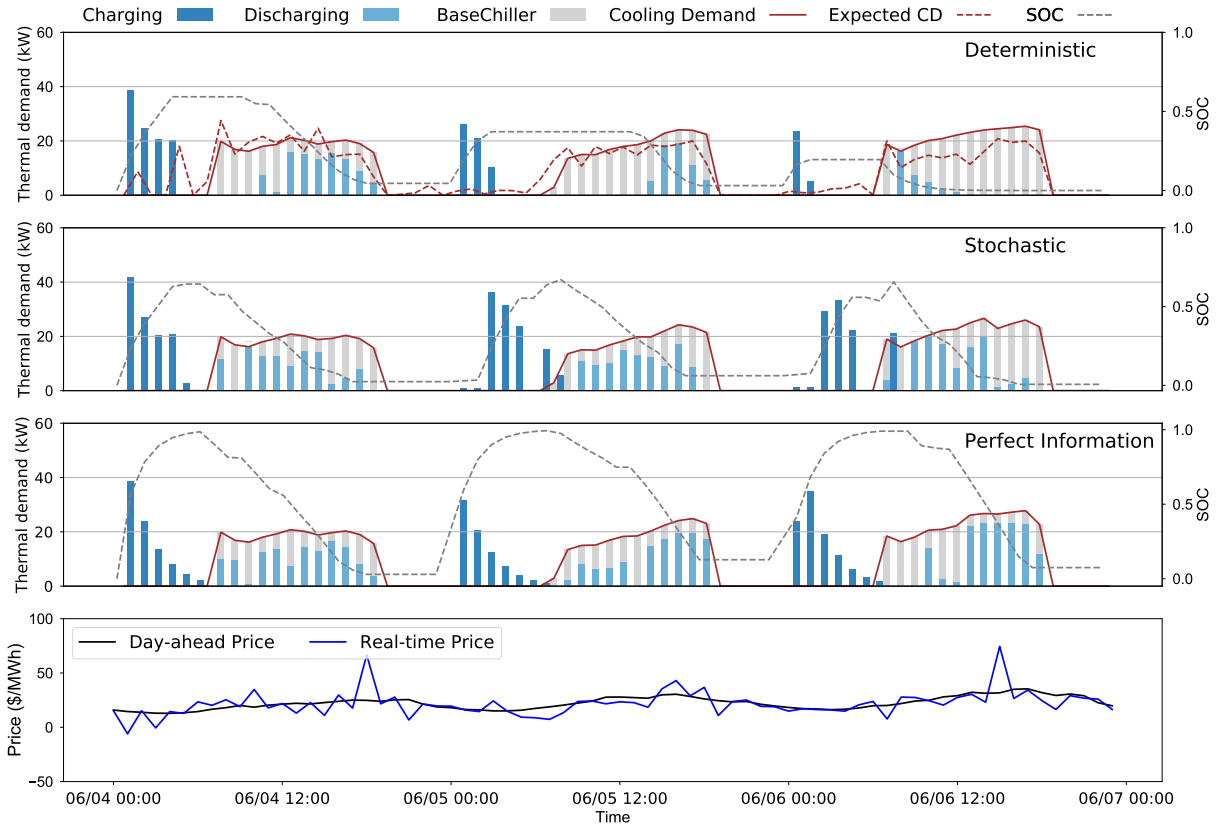

Figure 10: Detailed performance of real-time operation with stochastic, deterministic, and perfect information (Validation No. 11).

the buildings needed to charge during early morning hours if there were not a great amount of thermal energy stored in TES. In contrast, the expected electric demand that the deterministic case used for decision making was lower than the peak demand limit during most of the operation hours except 18:00, therefore, the deterministic (green solid line) decided not to use the power for charging during the early morning hours that the aggregator purchased in the day-ahead planning. Instead, the deterministic case sold the power and made profits during the early morning hours as shown in the second subfigure of Fig. 9. During the operation, the deterministic case needed more power than it expected at an expensive price. In addition to that, its actual power was above the peak demand limit so that peak penalties were charged as well. When the perfect information (black solid line) was available, the buildings were perfectly able to charge enough energy to use it later during the operation hours when the real-time power prices spiked at 16:00 as shown in the top and the third subfigures. The stochastic case (red solid line) charged a small amount of thermal energy during early morning hours. As it charged less than the perfect information case, it could still sell a small portion of the purchased electricity back to the grid. In addition to that, its performance showed similar to the perfect information case during the operation hours by discharging thermal energy to avoid peak limits. On this day, the stochastic case was able to not even make profits during early morning hours but also avoid peak limits. The findings demonstrate why the deterministic case showed longer tails at the probability distribution in Fig. 6 and brighter colors (higher costs) at the heatmap for penalty charges in Fig. 7.

Fig. 10 illustrates the detailed charging and discharging strategy differences of one specific building having the same control response function among different implementations. The top subfigure represents the TES operation of the deterministic case with the actual cooling demand (brown solid line), expected

cooling demand (brown dashed line), charged thermal energy (blue bar), discharged thermal energy (skyblue bar), heat transfer rate from base chiller (grey bar), and state of charge of the TES (grey dashed line). We observed that the expected cooling demand that the deterministic case used for decision making showed a similar pattern as the actual cooling demand, however, on June 6th, it was expected to be 5-10 kW lower than the actual demand. The failure to expect close to the actual cooling demand led the controller to charge (blue bar) less so that the deterministic case could not discharge (skyblue bar) when the real-time power price spiked during the day. As for the stochastic case, it charged more than the deterministic case as it considered a wide variability based on its expected cooling demand. The discharging operation was made when the power price was relatively lower. The perfect information case tended to charge until almost the maximum state of charge (grey dashed line) during early morning hours and spent most of them during the operation hours so that it was able to fully escape the risk from the high real-time power prices. Overall, the detailed performance results provide insights to explain how the failure in planning and operation could affect building performance. The stochastic performance was not fully able to escape the risk from the high spiking real-time power price, however, the control performance showed a similar pattern as the perfect information. It demonstrated the value added by considering a wide-range of future scenarios for decision-making.

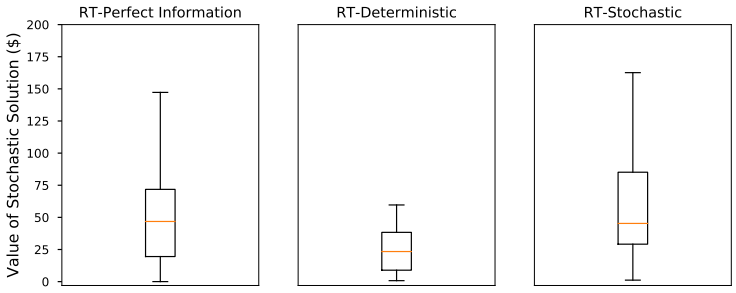

Figure 11: Value of Stochastic Solution in Day-ahead planning.

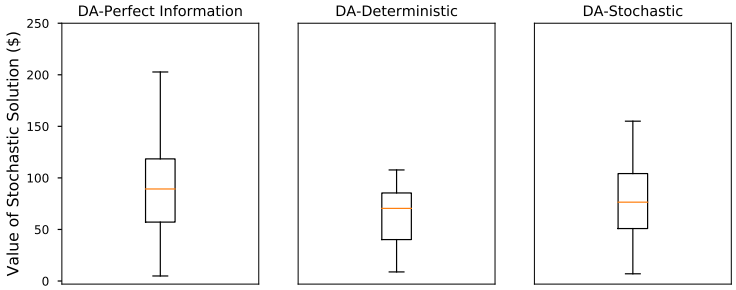

Figure 12: Value of Stochastic Solution in real-time operation.

Fig. 11 and Fig. 12 show the box plots of the value of the stochastic solution over the validation scenarios to highlight the benefits by applying the stochastic model rather than the deterministic model for the aggregator's portfolio. Value of Stochastic Solution (VSS) is defined as the difference between the mean value solution and the recourse problem to highlight the benefits of the stochastic model. The deterministic model of this work can represent the mean value solution as it applied the mean value of the forecasting model. The VSS was ranged from near zero to \$150 and the mean value of VSS was around \$20-50 in Fig. 11. The VSS in the real-time operation was \$200 at maximum and it is expected to achieve higher benefits at around \$50-80 in Fig. 12. Thus, it was observed that applying a stochastic model in real-time operation is more beneficial for aggregator's profits. It is also interesting to note that when deterministic controllers are used in either the RT or DA settings, the VSS range, median, and average VSS was lower. Thus, the capabilities of the stochastic framework is somewhat constrained when it is not used in both periods.

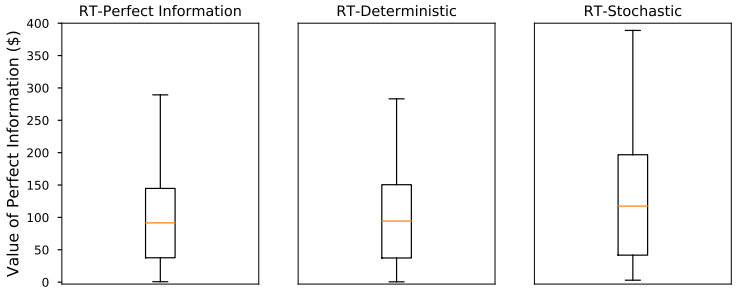

Figure 13: Value of perfect information in Day-ahead planning.

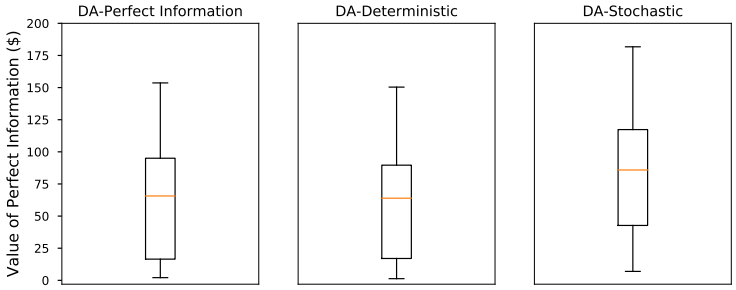

Figure 14: Value of perfect information in real-time operation.

Fig. 13 and Fig. 14 illustrate the box plot of the value of perfect information to highlight the possible gains by having perfect information rather than the mean value of expected scenarios ("Deterministic"). The value of perfect information was twice higher than the VSS. Thus, it is expected that the aggregator could benefit greatly from reducing uncertainty by gathering more information and improving forecasts close to perfect information.

7. Conclusion and discussion

This paper addresses how the quality of information could influence the overall performance of the supervisory controller to highlight the potential of the stochastic control framework. In this work, building demands, weather conditions, and real-time power prices are considered as the uncertain information for the aggregator when decision-making. We considered three levels of information with "Deterministic" (mean value of forecasting model), "Stochastic" (a set of uncertain forecasting scenarios), and "Perfect information" when decision-making. The proposed control framework is developed based on our previous work to consider the uncertainties in the day-ahead planning as well as in the real-time model predictive controller. Simulation case studies with 50 validation scenarios were carried out to quantitatively analyze the performance of the aggregator with 30 buildings in terms of total operation costs, building performance, and building side demand flexibility.

The distribution of the total operating costs in case studies showed that the lack of information which is to possess the mean value of forecasts could result in higher probabilities for larger expenditures. In addition, the forecasting ability with various future scenarios was financially beneficial in both day-ahead planning and real-time operation. The quality of the information in real-time operation has a decisive influence on total operating costs and overall performance to be under peak limit. From the heatmap analysis, it was highlighted that gathering more information and improving the quality of information would be helpful to avoid the penalty charges.

The detailed performance explored through the one day snapshots demonstrated how the decision could be different when the aggregator used one expected mean value scenario versus multiple uncertain scenarios. The stochastic model could benefit from considering a wide range of scenarios over the deterministic model. However, the limits of the proposed stochastic control framework were also observed from the detailed performance results for the real-time operation. The deterministic and stochastic cases made similar decisions when the expected demand was lower than the peak demand limit. This failure in the real-time operation led the aggregator to pay for the penalty charges and expensive balancing costs. Even though the stochastic control framework was able to foresee much of the potential volatility, the current framework is essentially risk-neutral and weights all scenarios equally. Thus, it did not avoid the uncertain scenario with expected expensive values at the tail aggressively, and incurred similar costs as the deterministic case.

From the VSS analysis, it was observed that the stochastic model in real-time operation could bring more financial benefits to aggregator than applying it in day-ahead planning. We also found the benefits of improving forecasts for the control framework would increase dramatically as it is close to perfect information.

Overall, the results show that it was advantageous to use the stochastic framework in both day-ahead and real-time settings. Considering uncertainties in both settings showed marked improvement over all cases that included a deterministic controller. This performance improvement was achieved despite the relatively large variation in scenarios (e.g., see Fig. 4, which suggests that more information—even if fairly uncertain—can be better than a deterministic model. This conclusion motivates continued pursuit of stochastic decision-making and control frameworks to enable future smart, grid-interactive buildings.

In future work, we plan to explore the risk-based objectives through this stochastic framework. Even though the stochastic approach considered the variance of the forecasting model, it was not able to fully comprehend extreme scenarios at the tails, which may lead to large costs. In the current risk-neural format, the expected profit was maximized even though the solution might include some probability of low profits or even substantial losses. Thus, future work considering a risk-based approach would be an important extension.

Bibliography

[1] Transforming our world: The 2030 agenda for sustainable development. Tech. Rep.; United Nations; 2015. https://sdgs.un.org/publications/transforming-our-world-2030-agenda-sustainable-development-17981.

[2] Silva BN, Khan M, Han K. Towards sustainable smart cities: A review of trends, architectures, components, and open challenges in smart cities. Sustainable Cities and Society 2018;38:697–713. URL: https://www.sciencedirect.com/science/article/pii/S2210670717311125. doi:https://doi.org/10.1016/j.scs.2018.01.053.

[3] Chen TM. Smart grids, smart cities need better networks [editor's note]. IEEE Network 2010;24(2):2–3. doi:10.1109/MNET.2010.5430136.

[4] Atasoy T, Akınç HE, Erçin
. An analysis on smart grid applications and grid integration of renewable energy systems in smart cities. In: 2015 International Conference on Renewable Energy Research and Applications (ICRERA). 2015, p. 547–50. doi:10.1109/ICRERA.2015.7418473.

[5] andAngelina LaRose SN. Annual energy outlook 2021 with projections to 2050. Tech. Rep.; The U.S. Energy Information Administration (EIA); 2021.

[6] Zeng B, Zhang J, Yang X, Wang J, Dong J, Zhang Y. Integrated planning for transition to low-carbon distribution system with renewable energy generation and demand response. IEEE Transactions on Power Systems 2014;29(3):1153–65. doi:10.1109/TPWRS.2013.2291553.

[7] Cara Carmichael RE, Taylor E. Grid-interactive efficient buildings made easy: A gsa building manager's guide to low- and no-cost geb measures. Tech. Rep.; U.S. Department of Energy, Office of Energy Efficiency and Renewable Energy, Building Technologies Office; 2021. https://rmi.org/insight/grid-interactive-efficient-buildings-made-easy/.

[8] Aduda K, Labeodan T, Zeiler W, Boxem G. Demand side flexibility coordination in office buildings: A framework and case study application. Sustainable Cities and Society 2017;29:139–58. URL: https://www.sciencedirect.com/science/article/pii/S2210670716301937. doi:https://doi.org/10.1016/j.scs.2016.12.008.

[9] Mbungu NT, Bansal RC, Naidoo R, Miranda V, Bipath M. An optimal energy management system for a commercial building with renewable energy generation under real-time electricity prices. Sustainable Cities and Society 2018;41:392–404. URL: https://www.sciencedirect.com/science/article/pii/S2210670717316384. doi:https://doi.org/10.1016/j.scs.2018.05.049.

[10] Mirakhorli A, Dong B. Market and behavior driven predictive energy management for residential buildings. Sustainable Cities and Society 2018;38:723–35. URL: https://www.sciencedirect.com/science/article/pii/S221067071731435X. doi:https://doi.org/10.1016/j.scs.2018.01.030.

[11] Connor P, Axon C, Xenias D, Balta-Ozkan N. Sources of risk and uncertainty in uk smart grid deployment: An expert stakeholder analysis. Energy 2018;161. doi:10.1016/j.energy.2018.07.115.

[12] Jankauskas V, Rudzkis P, Kanopka A. Risk factors for stakeholders in renewable energy investments. Energetika 2014;60. doi:10.6001/energetika.v60i2.2935.

[13] Jufri F, Widiputra V, Jung J. State-of-the-art review on power grid resilience to extreme weather events: Definitions, frameworks, quantitative assessment methodologies, and enhancement strategies. Applied Energy 2019;239:1049–65. doi:10.1016/j.apenergy.2019.02.017.

[14] Yu MG, Pavlak GS. Two-stage stochastic planning for control of building thermal energy storage portfolios with transactive controls. In: 2020 American Control Conference (ACC). 2020, p. 2339–44. doi:10.23919/ACC45564.2020.9147670.

[15] Yu MG, Pavlak GS. Assessing the performance of uncertainty-aware transactive controls for building thermal energy storage systems. Applied Energy 2021;282:116103. URL: http://www.sciencedirect.com/science/article/pii/S0306261920315233. doi:https://doi.org/10.1016/j.apenergy.2020.116103.

[16] Venkatesh Chinde Adam Hirsch WL, Florita AR. Simulating dispatchable grid services provided by flexible building loads: State of the art and needed building energy modeling improvements. Building Simulation 2021;32:441–462. doi:10.1007/s12273-020-0687-1.

[17] Zhang L, Wen J, Li Y, Chen J, Ye Y, Fu Y, et al. A review of machine learning in building load prediction. Applied Energy 2021;285:116452. URL: https://www.sciencedirect.com/science/article/pii/S0306261921000209. doi:https://doi.org/10.1016/j.apenergy.2021.116452.

[18] Ahmad A, Hassan M, Abdullah M, Rahman H, Hussin F, Abdullah H, et al. A review on applications of ann and svm for building electrical energy consumption forecasting. Renewable and Sustainable Energy Reviews 2014;33:102–9. URL: https://www.sciencedirect.com/science/article/pii/S1364032114000914. doi:https://doi.org/10.1016/j.rser.2014.01.069.

[19] Ahmad T, Chen H. A review on machine learning forecasting growth trends and their real-time applications in different energy systems. Sustainable Cities and Society 2020;54:102010. URL: https://www.sciencedirect.com/science/article/pii/S2210670719335516. doi:https://doi.org/10.1016/j.scs.2019.102010.

[20] Yang R, Hao J, Jiang H, Jin X. Machine-learning-driven, site-specific weather forecasting for grid-interactive efficient buildings: Preprint 2020;URL: https://www.osti.gov/biblio/1669587.

[21] Chan S, Tsui K, Wu H, Hou Y, Wu YC, Wu FF. Load/price forecasting and managing demand response for smart grids: Methodologies and challenges. IEEE Signal Processing Magazine 2012;29(5):68–85. doi:10.1109/MSP.2012.2186531.

[22] Huang CM, Huang CJ, Wang ML. A particle swarm optimization to identifying the armax model for short-term load forecasting. IEEE Transactions on Power Systems 2005;20(2):1126–33. doi:10.1109/TPWRS.2005.846106.

[23] Guo Q, Nojavan S, Lei S, Liang X. Economic-environmental analysis of renewable-based microgrid under a cvar-based two-stage stochastic model with efficient integration of plug-in electric vehicle and demand response. Sustainable Cities and Society 2021;75:103276. URL: https://www.sciencedirect.com/science/article/pii/S2210670721005527. doi:https://doi.org/10.1016/j.scs.2021.103276.

[24] Pan Z, Yu T, Li J, Qu K, Chen L, Yang B, et al. Stochastic transactive control for electric vehicle aggregators coordination: A decentralized approximate dynamic programming approach. IEEE Transactions on Smart Grid 2020;:1–.

[25] z. liu , Wu Q, Shahidehpour M, Li C, Huang S, Wei W. Transactive real-time electric vehicle charging management for commercial buildings with pv on-site generation. IEEE Transactions on Smart Grid 2019;10(5):4939–50. doi:10.1109/TSG.2018.2871171.

[26] Mehrjerdi H, Rakhshani E. Optimal operation of hybrid electrical and thermal energy storage systems under uncertain

loading condition. Applied Thermal Engineering 2019;160:114094. doi:10.1016/j.applthermaleng.2019.114094.
[27] Wanjiru EM, Sichilalu SM, Xia X. Model predictive control of heat pump water heater-instantaneous shower powered with integrated renewable-grid energy systems. Applied Energy 2017;204:1333–46. URL: https://www.sciencedirect.com/science/article/pii/S0306261917305342. doi:https://doi.org/10.1016/j.apenergy.2017.05.033.
[28] Krishnan Prakash A, Zhang K, Gupta P, Blum D, Marshall M, Fierro G, et al. Solar+ optimizer: A model predictive control optimization platform for grid responsive building microgrids. Energies 2020;13(12). URL: https://www.mdpi.com/1996-1073/13/12/3093. doi:10.3390/en13123093.
[29] Gholamzadehmir M, Del Pero C, Buffa S, Fedrizzi R, Aste N. Adaptive-predictive control strategy for hvac systems in smart buildings – a review. Sustainable Cities and Society 2020;63:102480. URL: https://www.sciencedirect.com/science/article/pii/S2210670720307009. doi:https://doi.org/10.1016/j.scs.2020.102480.
[30] Kumar R, Wenzel M, ElBsat M, Risbeck M, Drees K, Zavala V. Stochastic model predictive control for central hvac plants. Journal of Process Control 2020;90:1–17. doi:10.1016/j.jprocont.2020.03.015.
[31] Zhang Y, Meng F, Wang R, Zhu W, Zeng XJ. A stochastic mpc based approach to integrated energy management in microgrids. Sustainable Cities and Society 2018;41:349–62. URL: https://www.sciencedirect.com/science/article/pii/S2210670718303378. doi:https://doi.org/10.1016/j.scs.2018.05.044.
[32] Garifi K, Baker K, Touri B, Christensen D. Stochastic model predictive control for demand response in a home energy management system. In: 2018 IEEE Power Energy Society General Meeting (PESGM). 2018, p. 1–5. doi:10.1109/PESGM.2018.8586485.
[33] Ferrarini L, Mantovani G, Costanzo GT. A distributed model predictive control approach for the integration of flexible loads, storage and renewables. In: 2014 IEEE 23rd International Symposium on Industrial Electronics (ISIE). 2014, p. 1700–5. doi:10.1109/ISIE.2014.6864871.
[34] Chen Y, Hu M. Swarm intelligence–based distributed stochastic model predictive control for transactive operation of networked building clusters. Energy and Buildings 2019;198. doi:10.1016/j.enbuild.2019.06.010.
[35] Henze G, Felsmann C, Knabe G. Evaluation of optimal control for active and passive building thermal storage. International Journal of Thermal Sciences 2004;43:173–83. doi:10.1016/j.ijthermalsci.2003.06.001.
[36] Luetkepohl H. The New Introduction to Multiple Time Series Analysis. 2005. ISBN 978-3-540-40172-8. doi:10.1007/978-3-540-27752-1.
[37] Seabold S, Perktold J. statsmodels: Econometric and statistical modeling with python. In: 9th Python in Science Conference. 2010,.
[38] Energy market. https://www.pjm.com/markets-and-operations/energy.aspx; 2019. Accessed: 2021-10-15.